Methane Sensing with a Tungsten-Calix[4]arene-Based Conducting Polymer

*Ruqiang Lu, Shaoxiong Lennon Luo, Qilin He, Alberto Concellón, and Timothy M. Swager**

Dr. R. Lu, S. L. Luo, Q. He, Dr. A. Concellón, Prof. T. M. Swager

Department of Chemistry, Massachusetts Institute of Technology, Cambridge, MA 02139, USA.

E-mail: tswager@mit.edu

Keywords: methane sensor, calixarene, conducting polymer, host-guest interaction

Abstract: The detection of methane is important for industry, environment and our daily life, but is made challenging by its inert nature. Herein, we use a tungsten-capped calix[4]arene-based p-doped conducting polymer with hexafluorophosphate or perchlorate counter-anions as a transducer to detect methane. The host-guest interaction between calixarene moieties within the polymer chain and methane molecules leads to the resistance variation of the polymer. The experimental limit of detection (LoD) of methane for the polymer-based sensor was demonstrated to be less than 50 ppm at room temperature, and the extrapolated theoretical LoD of 2 ppm represents exceptional sensitivity to methane. Furthermore, the discrimination of methane from interfering volatile organic compounds (VOCs) was achieved by exploiting a sensor array using complementary chemiresistors and principle component analysis.

1. Introduction

Methane, the simplest alkane, is the main component in natural gas. It has been widely used as fuel for industry and domestic heating/cooking.[1] Methane is highly flammable and explodes when ignited at concentrations from 4.6% to 16.2% by volume under atmospheric conditions.[2] These features make the transport and the use of methane hazardous. Beyond this latter issue, methane is also a greenhouse gas with 25 times the effect of similar quantities of CO_2.[3] As a result, new sensitive detection schemes for methane emissions are of interest

for safety as well as environmental protection. However, owing to the inert properties of methane, its detection is challenging especially at trace levels. Present technologies used to detect methane include gas chromatography and metal oxide-based sensors. Gas chromatography analysis is sensitive and can detect methane at the low ppm level,[4] but suffers from high cost and complicated operations. Metal oxide-based methane sensors lack selectivity and usually require high temperature to oxidize methane,[5] which leads to power consumption and the risk of explosions. There are limited examples of the detection of methane at room temperature.[6] As a result, there remains a need for low power and cost methane sensors that exhibit high sensitivity.

Supramolecular host-guest interactions have demonstrated utility in gas sensor designs.[7] Calixarenes, which are macrocycles based on phenols connected in the 2,5-positions by methylenes, are an exceptionally versatile family of supramolecular hosts.[8] The most common calixarenes are calix[4-6]arenes and calix[8]arene, which display equilibrating conformations.[8h, 8i] Calix[4]arene, for example, has four possible conformations including the cone, partial cone, 1,2-alternate, and 1,3-alternate. To enforce rigidity to create a pre-organized receptor, a tungsten cap can lock calix[4]arene in a cone structure.[9] These conformationally rigid metallocalixarenes have been proved to be good hosts for organic small molecules such as benzene, toluene and dimethyl sulfoxide.[9a-c, 10] Atwood and co-workers had also previously reported that *p*-tert-butylcalix[4]arene binds methane,[11] thereby revealing the potential of calixarenes in methane sensing.

Herein, we employ a rigid tungsten-capped calix[4]arene-based p-doped conducting polymer with PF_6^- or ClO_4^- counter-anions as a transducer to detect methane at room temperature. The host-guest interaction between calixarene moieties and methane molecules leads to small structural and dielectric variations that trigger resistance changes of the polymer. We achieve experimental and theoretical limits of methane detection (LoD) of < 50 ppm and 2 ppm, respectively. These values are exceptionally low values for supramolecular

interaction-based methane sensors. Furthermore, the selective detection of methane was achieved by using a sensor array including complementary selectors/single-walled carbon nanotubes based sensors.

2. Results and Discussion

2.1. Properties of monomer

The monomer (**M**) and the conducting polymer used in this study were synthesized as described in a previous report with modifications.[9a] Single crystals of the monomer suitable for X-ray analysis were obtained by phase transfer of methanol into the solution of the monomer in dichloromethane (Table S1 and Figure 1b). One of two possible conformers of **M** (Figure S1), **M1**, was observed in the single crystal. The tungsten-capped calixarene moiety within conformer **M1** shows a bowl-shaped geometry with the C14−C14 and C24−C24 distances of 7.45 and 10.21 Å (Figure 1b). This cavity can accommodate methane that has a kinetic diameter of 3.8 Å.[12] The binding energy between **M1** and methane was calculated to be 8.32 kcal/mol (see supporting information for details), revealing the strong interaction between the host molecule and methane. The host-guest interaction between calixarene and methane leads to the structural variations of the calixarene from its guest free structure. Specifically, we predict based on computational results a pinching of the structure with the C14−C14 distance increasing from 7.13 to 7.17 Å and C24−C24 distance decreasing from 10.27 to 10.21 Å (Figure 1c). The structural changes also lead to the slight change in molecular orbital energies. In particular, the lowest unoccupied molecular orbital of **M1**+methane complex is 0.05 eV lower than that of **M1** (Figure 1d). The highest occupied molecular orbitals of **M1**+methane complex and **M1** are largely unchanged with methane binding. The binding energy between **M2** and methane was estimated to be 7.46 kcal/mol. The conformer **M2** shows similar trend in changes of geometries and molecular energies to those of **M1** when interacts with methane (Figure S1). These variations in structure and electronic properties of **M** resulting from the host-guest interactions can translate to the

conductivity changes when this monomer is incorporated within a conducting polymer backbone.

2.2. Synthesis and characterization of conducting polymer

The cyclic voltammogram and electrochemical polymerization of the calixarene monomer was performed in dichloromethane solution using Bu_4NPF_6 or Bu_4NClO_4 as the electrolyte, a Ag/Ag^+ reference electrode, and a 5 μm interdigitated electrode as a working electrode (Figure S2). The surface deposited polymer with PF_6^- or ClO_4^- as the counter-ions was potentiostatically synthesized at 1.5 V vs Ag/Ag^+. The consumed charge was limited 24.7 mC for all polymerizations to ensure similar amounts of polymer are deposited (Figure S2b and S2c). The resulting black film is amorphous as revealed by wide-angle X-ray diffraction, wherein no defined diffraction peaks are observed (Figure S3). Scanning electron microscope (SEM) reveals a surface morphology with microspheroid polymer aggregates (Figures 2a and 2c), which provides a beneficial large surface area for interaction with methane gas.[13] The polymer film was also characterized by X-ray photoelectron spectroscopy (XPS). All of the expected atoms were confirmed for both the counter-anions and the polymer (Figures 2b and 2d). The doping levels (anion/repeat unit[14]), estimated from the high-resolution XPS scans (Table S2), are 0.91 ± 0.04 and 0.89 ± 0.15 for the polymer with PF_6^- and ClO_4^- as counter-ions. The initial resistance of our devices is in the range of 250−800 Ω for the polymer with PF_6^- or ClO_4^- as counter-anions.

2.3. Sensing performance

The sensing performance as a function of the two polymer compositions was evaluated in dry air at room temperature using testing scheme shown in Figure S4. Surprisingly, we found the responses of the both materials to methane increase with time. Specifically, the response ($\Delta R/R_0$, %) at 800 ppm methane increases from 0.035 ± 0.004% (day 1) to 0.745 ± 0.036% over 40 days for the PF_6^- containing polymer and from 0.091 ± 0.017% (day 1) to 1.946 ± 0.124% in 26 days for the polymer with ClO_4^- counter-ions (Figure 3a). The origin of this

change was investigated. We observed that the resistance of the conducting polymer also increased with time (Figure 3b), which may result from de-doping and/or de-composition of the polymer.[15] Fourier transform infrared spectroscopy (FT-IR) was performed (Figure 3c) to evaluate this process. The freshly as-prepared polymer inherits most of the characteristic IR absorptions of monomer. However, when oxidized (charged), the wavenumbers of the aromatic C−H stretch, the alkyl C−H stretch and the aromatic C=C stretch in the as-prepared PF_6^--containing conducting polymer shift from 3065 cm^{-1} to 3058 cm^{-1}, from 2917 cm^{-1} to 2925 cm^{-1} and from 1588 cm^{-1} to 1581 cm^{-1}, respectively, compared with those of monomer. These changes are consistent with delocalized carbocation character within the aromatic rings. Upon electrochemical (EC) de-doping (reduction), the polymer shows IR absorptions more similar to the monomer as expected for the less charged state. The polymer stored in ambient conditions for 8 months has the similar characteristic IR absorption to that of EC-de-doping polymer, suggesting that de-doping occurs when the polymer is stored in air with relative humidity of 30−50%. It has been previously shown in other conducting polymers that moisture may act as a reducing species to reduce the bipolarons to polaron and neutral states.[16] However, the IR of the atmospherically reduced material also displays new peaks around 3250 cm^{-1} and 1643 cm^{-1}, revealing that the polymer also de-composed with time. Specifically, these species suggest that new ROH and carbonyl groups are produced. To clarify which process dominated in enhancing the response of the polymer to methane, the methane response of the polymer with different doping levels controlled by electro-chemical method[17] was tested. The response to methane largely increases with the lowering of doping levels (Figure S5). Specifically, the methane (800 ppm) responses are 0.043 ± 0.022%, 0.103 ± 0.027%, 0.122 ± 0.022 and 0.089 ± 0.017% for doping levels of 0.89 ± 0.15, 0.20 ± 0.05, 0.18 ± 0.04 and 0.11 ± 0.01 (Table S4), respectively. The lower response at a doping level of 0.11 is likely the result of the very high resistivity of these films. However, it is worth noting that the response enhanced by electrochemically controlled doping level is not as significant

as that achieved by long term exposure to ambient atmosphere. These results indicate that the de-doping and de-composing processes both contribute to the increasing response of the polymer to methane. A clue to the origin of the increased response to methane is that we observe a concomitate increase in the hydrophobicity of the polymer films as evidenced by the increasing water contact angles (Figure 3d). This increasing hydrophobicity is characteristic of de-doping and the lower charge density in the polymer backbone. This change may facilitate the interaction between calixarene moieties and non-polar methane molecules and/or a decreased carrier density can result in higher sensitivity to energetic heterogenicity caused by partial binding of methane to some of the calixarene hosts. The faster environmental aging of the ClO_4^--containing polymer relative to the PF_6^--containing material reveals that the counter ions have a role in this process.

The sensing performance of polymers containing PF_6^- and ClO_4^- counter-ions on day 40 and day 26 is shown in Figure 4. The response to methane changes linearly with methane concentrations below 1000 ppm and displays indications of saturation for both anion containing polymers at methane concentrations higher than 1000 ppm. The linearly fits to the concentration-dependent response shows 8.9×10^{-4} % response change per ppm for PF_6^--containing polymer and 2.5×10^{-3} % response change per ppm for ClO_4^--containing polymer (Figure S6). A clearly observable response is apparent at 50 ppm methane for both materials. The theoretical limits of detection are estimated to be 22 ppm for PF_6^--containing polymer and 2 ppm for ClO_4^--containing polymer with the signal-to-noise ratio (S/N) > 3. These limits represent a clear advance in methane detection in terms of sensitivity and the simplicity of the measurements. Additionally, the fast response and recovery of the sensor[6a, 6c, 6f, 18] are calculated to be 56 s and 102 s at 800 ppm methane for ClO_4^--containing polymer (the response and recovery times are the time periods required to response and recovery to 90% of $\Delta R/R_0$). Unfortunately, the sensors showed no response toward methane in wet air with even

low relative humidity of 20%−30%. As a result, a pre-drying column will be required to mitigate this humidity issue for real world applications.

The response of ClO_4^--containing polymer toward the volatile interfering species other than methane was also evaluated. The sensor shows a lower response to hexane than to methane at the concentration of 400 ppm. The response to benzene is comparable to that to methane. The response to 400 ppm toluene and xylene (200 ppm for *m*-xylene) is higher than that to methane. This trend is consistent with previous reported results obtained for the materials based on calixarenes and in general higher molecular weight molecules display increased partioning into organic layers.[19] To further achieve the selectivity, a sensor array with expanded recognition elements was exploited. The selectors of the array are shown in Table S5. The pentiptycene polymers (sensors S2–S4)[20] and cavitand calixarene molecules (sensors S5 and S6)[21] were proved to be efficient selectors for benzene-toluene-xylene (BTX) sensing. Compound **M** was also used as a selector (S7). For sensors S2–S4, selector polymers were mixed with SWCNT.[20] For sensors S5–S7, selector calixarenes were drop-casted onto the SWCNT layer. The details of device fabrications are shown in Experimental Section/Methods. Sensors S2–S7 show no response to 400 ppm methane. The responses of ClO_4^--containing polymer (S1) and S2–S7 to methane, hexane and BTX are summarized in Figure 5b. These sensing data were further treated with principle component analysis.[22] The response of methane was clearly separated from those of hexane and BTX (Figure 5c). The responses of BTX can also be well separated. Overall, the selective detection of methane was successfully achieved.

3. Conclusion

In summary, a conducting polymer with a tungsten-capped calix[4]arene within the polymer main chain has been shown to high sensitivity and fast response and recovery when used as a chemiresistive sensor for methane. The p-doped polymer with PF_6^- or ClO_4^- counter-ions shows an increasing response to methane over time, arising from the increasing

hydrophobicity resulting from the de-doping and de-composing processes of polymer over time. The empirical and theoretical LoD toward methane of the polymer with a ClO_4^- counter-ion on day 26 is < 50 ppm and about 2 ppm, respectively. A sensor array and PCA successfully discriminates methane from its possible interfering species. These results reveal the tungsten-capped calix[4]arene are efficient molecular recognition elements for the creation of methane detection materials. Further improvements in the humidity tolerance of methane detection using calixarene-based materials are the subject of ongoing investigations.

4. Experimental Section/Methods

Experimental details and methods. All chemicals were used as received unless otherwise noted. Electrochemical polymerizations and cyclic voltammograms were performed using a Biologic SP-150 potentiostat with a Pt wire as a counter electrode, an Ag/Ag^+ electrode as a reference electrode and an interdigitated electrode as a working electrode. The interdigitated electrode, purchased from Metrohm USA, has two interdigitated electrodes with 5 μm gaps and with two connection tracks, made of platinum, on a glass substrate. The glass substrate dimensions are L 22.8 × W 7.6 × H 0.7 mm. Glass slides (VWR microscope slides) used for preparation of electrodes for sensors S2−S7 were bath sonicated in acetone for 15 min and then dried with a stream of nitrogen. Using an aluminum mask, chromium (15 nm) followed by gold (50 nm) was deposited using a Thermal Evaporator (Angstrom Engineering), leaving a 1 mm gap between gold electrodes. Single crystal diffraction was recorded on a Bruker D8 Venture Kappa DUO four-circle diffractometer and a Bruker Photon3 CPAD detector. Scanning electron microscope (SEM) was performed on the Merlin and Crossbeam 540 Zeiss SEM. The polymer film was coated with 10 nm gold film. X-ray photoelectron spectroscopy (XPS) was recorded on a Thermo Scientific K-Alpha$^+$ XPS. X-ray diffraction (XRD) was performed with a SAXSLAB instrument equipped with a Rigaku 002 microfocus X-ray source (CuKα = 1.5409 Å) and a Dectris Pilatus 300K detector that moves from 100 mm to 1500 mm from the sample. The beam center and the *q* range were calibrated using the

diffraction peaks of silver behenate. Fourier transform–infrared (FT-IR) spectroscopy was performed on a Thermo Scientific Nicolet 6700 Fourier transform infrared spectrometer using an attenuated total reflectance (ATR) attachment with a Ge crystal. Resistance was measured by an Agilent Keysight 34970A potentiostat bearing a 34901A 20-channel multiplexer (2/4-wire) module. Gas flow rates of dry air and methane were controlled by MC-10SLPM-D/5M and MC-10SCCM-D/5M mass flow controllers (MFCs), respectively. Analyte gases (hexane, benzene, toluene, and *o*/*m*/*p*-xylenes) were generated by a FlexStream FlexBase module with precise temperature (±0.01 °C) and gas flow rate control (±1.5% of the reading).

Electrochemical studies. The electrochemical polymerizations and CVs were performed in dry dichloromethane with 0.78 mM monomer **M** and 0.1 M Bu_4NPF_6 or Bu_4NClO_4. The potential was held at 1.5 V vs Ag/Ag^+ for polymerizations. The consuming charge was limited 24.7 mC for all electrochemical polymerizations. The prepared polymer was dried under vaccum for 30 min before sensing measurements. For electrochemical de-doping, the freshly prepared polymer was washed with dichloromethane and then placed in a monomer-free dichloromethane solution (with 0.1 M Bu_4NClO_4) and treated with potentials of 1.0 V, 0.6 V and 0.2 V vs Ag/Ag^+ until the current was stable (after 5 min). The conducting polymer used for FT-IR measurements was prepared by using indium tin oxides (ITO) as the working electrode.

Device fabrications. For sensors S2−S4[20]: Polymer selector (10 mg) was dissolved in *o*-dichlorobenzene (*o*DCB, 10 mL) and the solution was sonicated in water bath for 10 min. To the polymer solution, 1 mg of SG65i SWCNT was added and the resulting mixture was chilled with ice and homogenized for 20 min using Qsonica Q125 Sonicator at 63W. Subsequently, the suspension was centrifuged for 30 min at 8000 g and allowed to stand overnight undisturbed. 1 µL of the polymer/SWCNT supernate was drop-casted in between the gold electrodes and dried at RT under house vacuum in a desiccator or vacuum oven. For sensors S5−S7: 1 µL of the SG65i SWCNT dispersion was drop-casted in between the gold

electrodes and dried at RT under house vacuum in a desiccator or vacuum oven. Calix[4]arene and 4-*tert*-butylcalix[4]arene selectors (5 mg) were dissolved in warm toluene (2 mL) and monomer **M** (5 mg) was dissolved in dichloromethane (2 mL). The solution was sonicated in water bath for 10 min. 1 µL of the selector solution was then drop-casted in between the gold electrodes and dried at RT under house vacuum in a desiccator or vacuum oven.

CCDC 2024225 contains the supplementary crystallographic data for this paper. These data can be obtained free of charge from The Cambridge Crystallographic Data Centre via www.ccdc.cam.ac.uk/data_request/cif.

Supporting Information

Supporting Information is available from the Wiley Online Library or from the author.

Acknowledgements

This work was supported by Eni S.p.A. through the MIT energy initiative and the National Science Foundation (DMR 1809740).

Received: ((will be filled in by the editorial staff))
Revised: ((will be filled in by the editorial staff))
Published online: ((will be filled in by the editorial staff))

References

[1] a) M. Götz, J. Lefebvre, F. Mörs, A. McDaniel Koch, F. Graf, S. Bajohr, R. Reimert, T. Kolb, *Renewable Energy* **2016**, *85*, 1371; b) B. C. H. Steele, *Nature* **1999**, *400*, 619.

[2] G. De Smedt, F. de Corte, R. Notelé, J. Berghmans, *J. Hazard. Mater.* **1999**, *70*, 105.

[3] Overview of Greenhouse Gases, https://www.epa.gov/ghgemissions/overview-greenhouse-gases. accessed 20 April 2020.

[4] J. R. Valentin, G. C. Carle, J. B. Phillips, *Anal. Chem.* **1985**, *57*, 1035.

[5] a) Y. G. Song, J. Y. Park, J. M. Suh, Y.-S. Shim, S. Y. Yi, H. W. Jang, S. Kim, J. M. Yuk, B.-K. Ju, C.-Y. Kang, *Chem. Mater.* **2019**, *31*, 207; b) K. S. V. Santhanam, N. N. N. Ahamed, *ChemEngineering* **2018**, *2*, 38/1.

[6] a) E. Lee, A. VahidMohammadi, Y. S. Yoon, M. Beidaghi, D.-J. Kim, *ACS Sens.* **2019**, *4*, 1603; b) A. H. Khoshaman, P. C. H. Li, N. Merbouh, B. Bahreyni, *Sens. Actuators B* **2012**, *161*, 954; c) G. Chimowa, Z. P. Tshabalala, A. A. Akande, G. Bepete, B. Mwakikunga, S. S. Ray, E. M. Benecha, *Sens. Actuators B* **2017**, *247*, 11; d) J. Liang, J. Liu, W. Li, M. Hu, *Mater. Res. Bull.* **2016**, *84*, 332; e) J. Liang, J. Liu, N. Li, W. Li, *J. Alloys Compd.* **2016**, *671*, 283; f) Z. Wu, X. Chen, S. Zhu, Z. Zhou, Y. Yao, W. Quan, B. Liu, *IEEE Sens. J.* **2013**, *13*, 777.

[7] a) T. M. Swager, *Angew. Chem., Int. Ed.* **2018**, *57*, 4248; b) S. Kumar, S. Chawla, M. C. Zou, *J. Inclusion Phenom. Macrocyclic Chem.* **2017**, *88*, 129.

[8] a) H.-W. Tian, Y.-C. Liu, D.-S. Guo, *Mater. Chem. Front.* **2020**, *4*, 46; b) R. Kumar, A. Sharma, H. Singh, P. Suating, H. S. Kim, K. Sunwoo, I. Shim, B. C. Gibb, J. S. Kim, *Chem. Rev.* **2019**, *119*, 9657; c) J. Harrowfield, *Chem. Commun.* **2013**, *49*, 1578; d) D.-S. Guo, Y. Liu, *Chem. Soc. Rev.* **2012**, *41*, 5907; e) J. Rebek, Jr., *Chem. Commun.* **2000**, 637; f) A. F. D. de Namor, R. M. Cleverley, M. L. Zapata-Ormachea, *Chem. Rev.* **1998**, *98*, 2495; g) D. Diamond, M. A. McKervey, *Chem. Soc. Rev.* **1996**, *25*, 15; h) C. D. Gutsche, *Top. Curr. Chem.* **1984**, *123*, 1; i) A. Ikeda, S. Shinkai, *Chem. Rev.* **1997**, *97*, 1713.

[9] a) A. Vigalok, T. M. Swager, *Adv Mater* **2002**, *14*, 368; b) A. Vigalok, Z. Zhu, T. M. Swager, *J. Am. Chem. Soc.* **2001**, *123*, 7917; c) F. Corazza, C. Floriani, A. Chiesi-Villa, C. Rizzoli, *Inorg. Chem.* **1991**, *30*, 4465; d) L. Giannini, E. Solari, A. Zanotti-Gerosa, C. Floriani, A. Chiesi-Villa, C. Rizzoli, *Angew. Chem. Int. Ed.* **1996**, *35*, 2825.

[10] Y. Zhao, T. M. Swager, *J. Am. Chem. Soc.* **2013**, *135*, 18770.

[11] P. K. Thallapally, K. A. Kirby, J. L. Atwood, *New J. Chem.* **2007**, *31*, 628.

[12] Ismail, A. F.; Khulbe, K. C.; Matsuura, T. J. S. S., Gas separation membranes. Switzerland: Springer, **2015**.

[13] a) Y. Shen, T. Yamazaki, Z. Liu, D. Meng, T. Kikuta, N. Nakatani, *Thin Solid Films* **2009**, *517*, 2069; b) G. J. Li, X. H. Zhang, S. Kawi, *Sens. Actuators B* **1999**, *60*, 64.

[14] a) P. Pfluger, G. B. Street, *J. Chem. Phys.* **1984**, *80*, 544; b) G. A. Sotzing, J. R. Reynolds, P. J. Steel, *Chem. Mater.* **1996**, *8*, 882.

[15] a) T. Nezakati, A. Seifalian, A. Tan, A. M. Seifalian, *Chem. Rev.* **2018**, *118*, 6766; b) A. G. MacDiarmid, *Angew. Chem., Int. Ed.* **2001**, *40*, 2581.

[16] a) W. Chun-Guey, C. Mei-Jui, L. Yii-Chung, *J. Mater. Chem.* **1998**, *8*, 2657; b) M. C. Magnoni, M. C. Gallazzi, G. Zerbi, *Acta Polym.* **1996**, *47*, 228; c) M. R. Andersson, Q. Pei, T. Hjertberg, O. Inganäs, O. Wennerström, J. E. Österholm, *Synth. Met.* **1993**, *55*, 1227.

[17] W. Yao, L. Shen, P. Liu, C. Liu, J. Xu, Q. Jiang, G. Liu, G. Nie, F. Jiang, *Mater. Chem. Front.* **2020**, *4*, 597.

[18] W. Li, J. Liang, J. Liu, L. Zhou, R. Yang, M. Hu, *Mater. Lett.* **2016**, *173*, 199.

[19] F. Wang, Y. Yang, T. M. Swager, *Angew. Chem., Int. Ed.* **2008**, *47*, 8394.

[20] S.-X. L. Luo, C.-J. Lin, K. H. Ku, K. Yoshinaga, T. M. Swager, *ACS Nano* **2020**, *14*, 7297.

[21] a) F. Wang, T. M. Swager, *J. Am. Chem. Soc.* **2011**, *133*, 11181; b) V. Schroeder, E. D. Evans, Y.-C. M. Wu, C.-C. A. Voll, B. R. McDonald, S. Savagatrup, T. M. Swager, *ACS Sens.* **2019**, *4*, 2101.

[22] S. Stewart, M. A. Ivy, E. V. Anslyn, *Chem. Soc. Rev.* **2014**, *43*, 70.

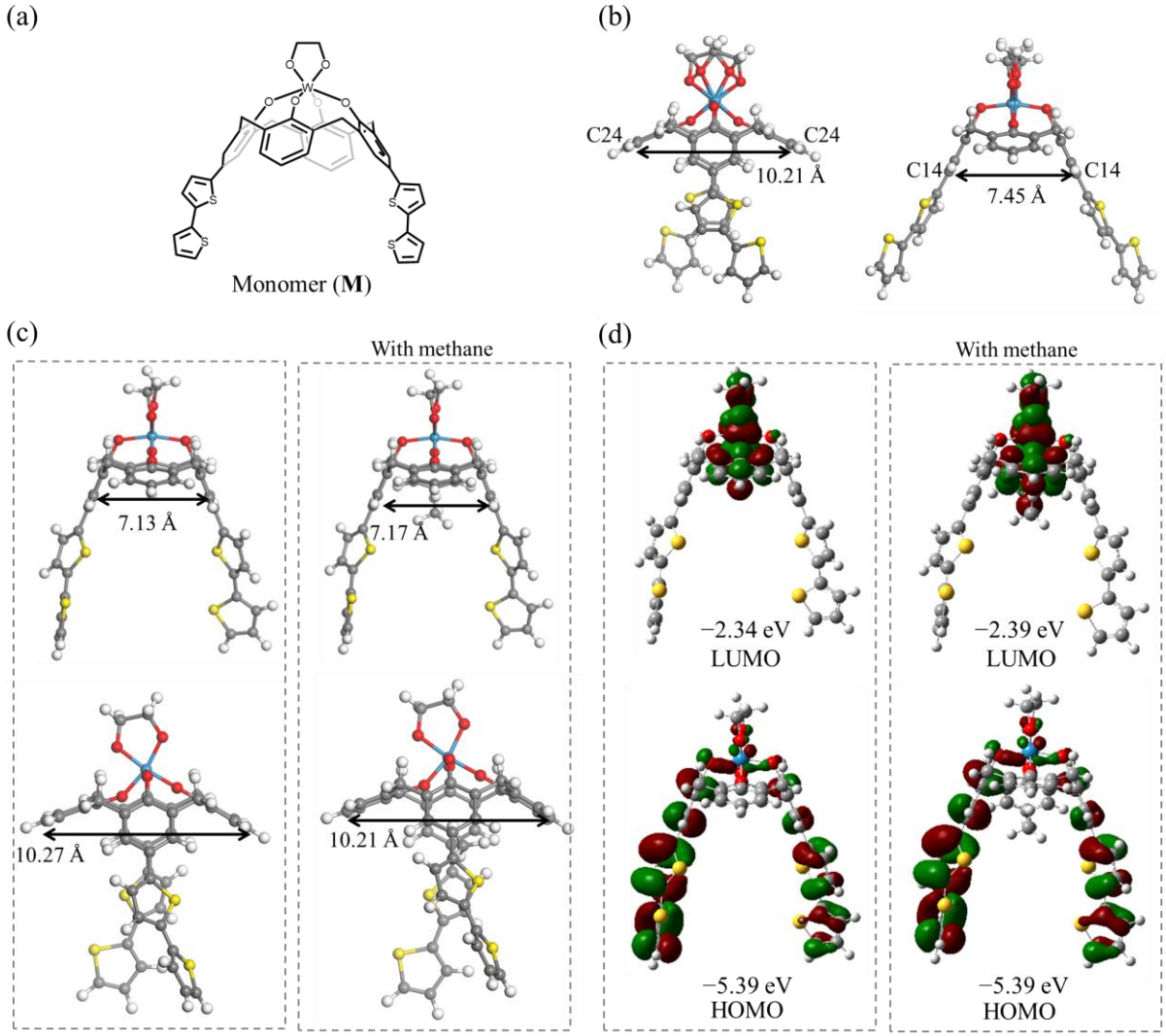

Figure 1. (a) Molecular and (b) single-crystal structures of **M** and **M1**. (c) Optimized structure and (d) molecular orbitals of **M1** and its complex with methane. The structures were optimized at the ωB97X-D/6-31G(d) level for C, H, O and S and ωB97X-D/LanL2DZ level for W. The electronic properties were further calculated at the B3LYP/6-311G(d) level for C, H, O and S and the B3LYP /LanL2DZ level for W.

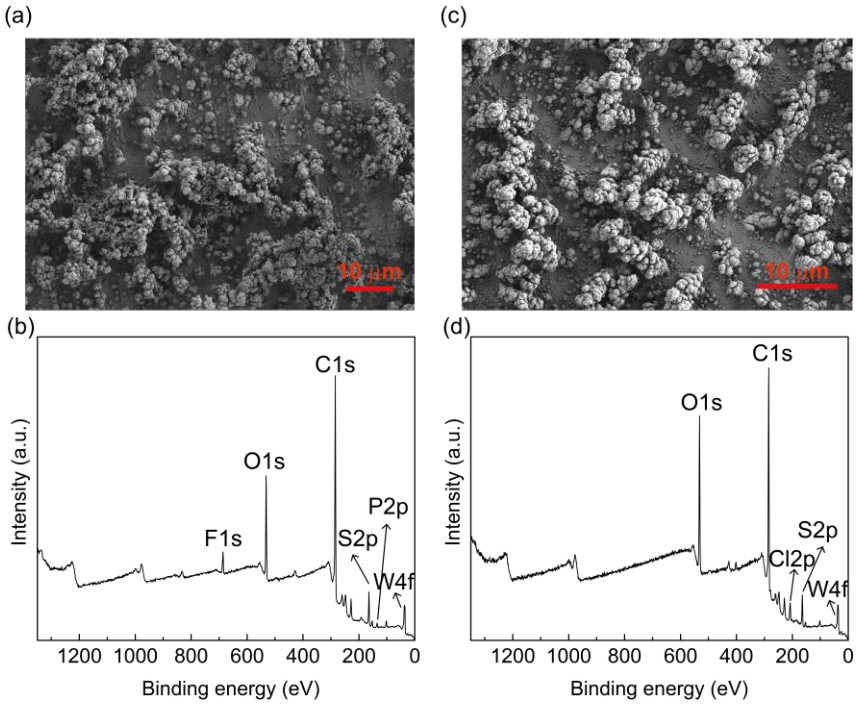

Figure 2. (a) SEM and (b) XPS survey scans of the polymer with PF_6^- as counter-ion. (c) SEM and (d) XPS survey scans of the polymer with ClO_4^- as counter-ion.

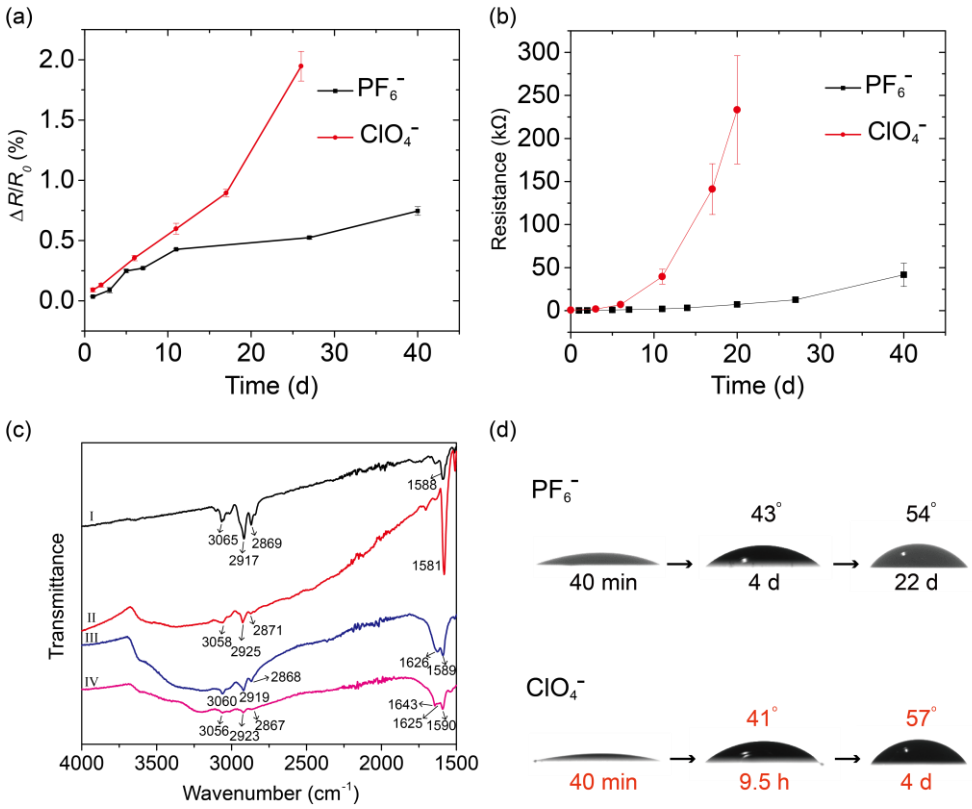

Figure 3. (a) Time-dependent response at 800 ppm methane concentration, (b) time-dependent resistance and (d) time-dependent water contact angles of polymers with PF_6^- and ClO_4^- as counter-ions. N ≥ 3. (c) IR spectra of monomer (I), freshly as-prepared polymer (II), EC-de-doping polymer (III, de-doping at −0.2 V vs Ag/Ag^+ for 5 min) and the polymer stored under ambient conditions for 8 months. Counter-anion: PF_6^-.

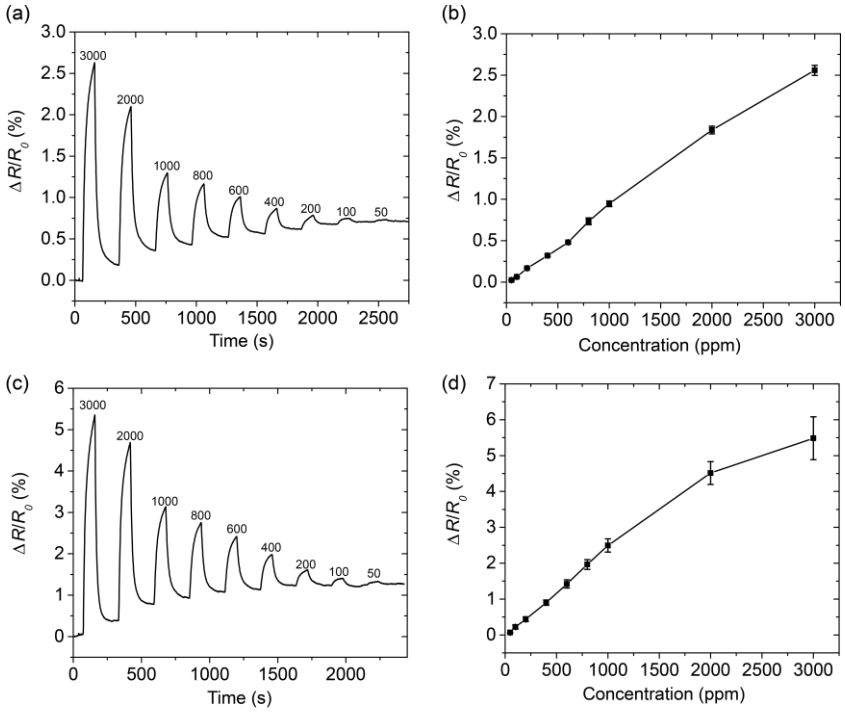

Figure 4. Concentration-dependent responses of (a, b) of the doped polymer with a PF_6^- counter-ion on day 40 (N ≥ 3) and similarly (c, d) for the polymer containing the ClO_4^- counter-ions on day 26 (N ≥ 3). The concentrations of methane are indicated in ppm values next to the respective peaks.

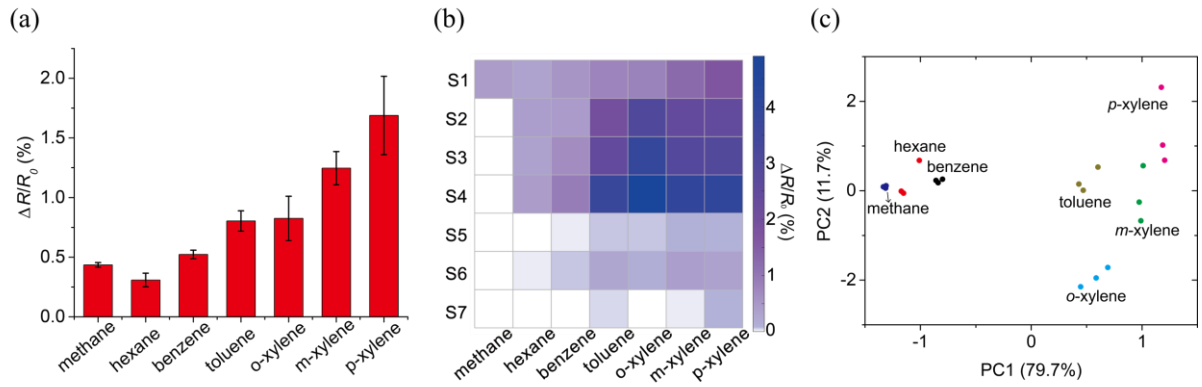

Figure 5. Response of (a) the doped polymer with a ClO_4^- counter-anion and (b) response patterns of the sensor array to hexane, benzene, toluene (400 ppm) and xylenes (400 ppm for *o*-xylene and *p*-xylene and 200 ppm for *m*-xylene) on day 17. Exposure time to the analytes in dry air is 100 s, N = 3. (c) PCA of the sensor array.